

World Journal of *Gastroenterology*

World J Gastroenterol 2023 February 7; 29(5): 766-907



EDITORIAL

- 766 Human leukocyte antigen antibodies and leukocyte antigen/killer-cell immunoglobulin-like receptor genes are important in transplant immunology in the liver
Muro M, Legaz I

OPINION REVIEW

- 773 Management of gastro-esophageal reflux disease: Practice-oriented answers to clinical questions
Frazzoni L, Fuccio L, Zagari RM

REVIEW

- 780 Transcriptome analysis creates a new era of precision medicine for managing recurrent hepatocellular carcinoma
Chiang CC, Yeh H, Lim SN, Lin WR
- 800 Impact of chronic liver disease on SARS-CoV-2 infection outcomes: Roles of stage, etiology and vaccination
Nevola R, Criscuolo L, Beccia D, Delle Femine A, Ruocco R, Imbriani S, Alfano M, Villani A, Russo A, Perillo P, Marfella R, Adinolfi LE, Sasso FC, Marrone A, Rinaldi L

MINIREVIEWS

- 815 Outcomes of COVID-19 among patients with liver disease
Vujčić I
- 825 Bone loss in chronic liver diseases: Could healthy liver be a requirement for good bone health?
Jadzic J, Djonic D
- 834 Liver involvement in patients with COVID-19 infection: A comprehensive overview of diagnostic imaging features
Ippolito D, Maino C, Vernuccio F, Cannella R, Inchingolo R, Dezio M, Faletti R, Bonaffini PA, Gatti M, Sironi S

ORIGINAL ARTICLE**Basic Study**

- 851 *Saccharomyces cerevisiae* prevents postoperative recurrence of Crohn's disease modeled by ileocecal resection in HLA-B27 transgenic rats
Valibouze C, Specca S, Dubuquoy C, Mourey F, M'Ba L, Schneider L, Titecat M, Foligné B, Genin M, Neut C, Zerbib P, Desreumaux P
- 867 Impact of endothelial nitric oxide synthase activation on accelerated liver regeneration in a rat ALPPS model
Masuo H, Shimizu A, Motoyama H, Kubota K, Notake T, Yoshizawa T, Hosoda K, Yasukawa K, Kobayashi A, Soejima Y

Retrospective Study

- 879** Convolutional neural network-based segmentation network applied to image recognition of angiodysplasias lesion under capsule endoscopy

Chu Y, Huang F, Gao M, Zou DW, Zhong J, Wu W, Wang Q, Shen XN, Gong TT, Li YY, Wang LF

Clinical Trials Study

- 890** Efficacy of dexamethasone and N-acetylcysteine combination in preventing post-embolization syndrome after transarterial chemoembolization in hepatocellular carcinoma

Simasingha N, Tanasoontrarat W, Claimon T, Sethasine S

LETTER TO THE EDITOR

- 904** Timing of biliary decompression for acute cholangitis

Yang J, Liu Y, Liu S

ABOUT COVER

Editorial Board Member of *World Journal of Gastroenterology*, Jian-Gao Fan, PhD, Professor and Director, Center for Fatty Liver Disease, Department of Gastroenterology, Xinhua Hospital, Shanghai Jiaotong University School of Medicine; Shanghai Key Laboratory of Children's Digestion and Nutrition, Shanghai 200092, China.
fattyLiver2004@126.com

AIMS AND SCOPE

The primary aim of *World Journal of Gastroenterology* (*WJG*, *World J Gastroenterol*) is to provide scholars and readers from various fields of gastroenterology and hepatology with a platform to publish high-quality basic and clinical research articles and communicate their research findings online. *WJG* mainly publishes articles reporting research results and findings obtained in the field of gastroenterology and hepatology and covering a wide range of topics including gastroenterology, hepatology, gastrointestinal endoscopy, gastrointestinal surgery, gastrointestinal oncology, and pediatric gastroenterology.

INDEXING/ABSTRACTING

The *WJG* is now abstracted and indexed in Science Citation Index Expanded (SCIE, also known as SciSearch®), Current Contents/Clinical Medicine, Journal Citation Reports, Index Medicus, MEDLINE, PubMed, PubMed Central, Scopus, Reference Citation Analysis, China National Knowledge Infrastructure, China Science and Technology Journal Database, and Superstar Journals Database. The 2022 edition of Journal Citation Reports® cites the 2021 impact factor (IF) for *WJG* as 5.374; IF without journal self cites: 5.187; 5-year IF: 5.715; Journal Citation Indicator: 0.84; Ranking: 31 among 93 journals in gastroenterology and hepatology; and Quartile category: Q2. The *WJG*'s CiteScore for 2021 is 8.1 and Scopus CiteScore rank 2021: Gastroenterology is 18/149.

RESPONSIBLE EDITORS FOR THIS ISSUE

Production Editor: *Ying-Yi Yuan*; Production Department Director: *Xiang Li*; Editorial Office Director: *Jia-Ru Fan*.

NAME OF JOURNAL

World Journal of Gastroenterology

ISSN

ISSN 1007-9327 (print) ISSN 2219-2840 (online)

LAUNCH DATE

October 1, 1995

FREQUENCY

Weekly

EDITORS-IN-CHIEF

Andrzej S Tarnawski

EDITORIAL BOARD MEMBERS

<http://www.wjgnet.com/1007-9327/editorialboard.htm>

PUBLICATION DATE

February 7, 2023

COPYRIGHT

© 2023 Baishideng Publishing Group Inc

INSTRUCTIONS TO AUTHORS

<https://www.wjgnet.com/bpg/gerinfo/204>

GUIDELINES FOR ETHICS DOCUMENTS

<https://www.wjgnet.com/bpg/GerInfo/287>

GUIDELINES FOR NON-NATIVE SPEAKERS OF ENGLISH

<https://www.wjgnet.com/bpg/gerinfo/240>

PUBLICATION ETHICS

<https://www.wjgnet.com/bpg/GerInfo/288>

PUBLICATION MISCONDUCT

<https://www.wjgnet.com/bpg/gerinfo/208>

ARTICLE PROCESSING CHARGE

<https://www.wjgnet.com/bpg/gerinfo/242>

STEPS FOR SUBMITTING MANUSCRIPTS

<https://www.wjgnet.com/bpg/GerInfo/239>

ONLINE SUBMISSION

<https://www.f6publishing.com>

Retrospective Study

Convolutional neural network-based segmentation network applied to image recognition of angiodysplasias lesion under capsule endoscopy

Ye Chu, Fang Huang, Min Gao, Duo-Wu Zou, Jie Zhong, Wei Wu, Qi Wang, Xiao-Nan Shen, Ting-Ting Gong, Yuan-Yi Li, Li-Fu Wang

Specialty type: Gastroenterology and hepatology

Provenance and peer review: Invited article; Externally peer reviewed.

Peer-review model: Single blind

Peer-review report's scientific quality classification

Grade A (Excellent): 0
Grade B (Very good): B
Grade C (Good): C
Grade D (Fair): 0
Grade E (Poor): 0

P-Reviewer: Garcia-Pola M, Spain; Morya AK, India

Received: September 25, 2022

Peer-review started: September 25, 2022

First decision: October 18, 2022

Revised: November 26, 2022

Accepted: January 11, 2023

Article in press: January 11, 2023

Published online: February 7, 2023



Ye Chu, Duo-Wu Zou, Jie Zhong, Wei Wu, Qi Wang, Xiao-Nan Shen, Ting-Ting Gong, Li-Fu Wang, Department of Gastroenterology, Shanghai Jiao Tong University School of Medicine, Ruijin Hospital, Shanghai 200025, China

Fang Huang, Min Gao, Yuan-Yi Li, Technology Platform Department, Jinshan Science & Technology (Group) Co., Ltd., Chongqing 401120, China

Corresponding author: Li-Fu Wang, MD, PhD, Chief Physician, Professor, Department of Gastroenterology, Shanghai Jiao Tong University School of Medicine, Ruijin Hospital, No. 197 Ruijin Er Road, Shanghai 200025, China. lifuwang@sjtu.edu.cn

Abstract

BACKGROUND

Small intestinal vascular malformations (angiodysplasias) are common causes of small intestinal bleeding. While capsule endoscopy has become the primary diagnostic method for angiodysplasia, manual reading of the entire gastrointestinal tract is time-consuming and requires a heavy workload, which affects the accuracy of diagnosis.

AIM

To evaluate whether artificial intelligence can assist the diagnosis and increase the detection rate of angiodysplasias in the small intestine, achieve automatic disease detection, and shorten the capsule endoscopy (CE) reading time.

METHODS

A convolutional neural network semantic segmentation model with a feature fusion method, which automatically recognizes the category of vascular dysplasia under CE and draws the lesion contour, thus improving the efficiency and accuracy of identifying small intestinal vascular malformation lesions, was proposed. Resnet-50 was used as the skeleton network to design the fusion mechanism, fuse the shallow and depth features, and classify the images at the pixel level to achieve the segmentation and recognition of vascular dysplasia. The training set and test set were constructed and compared with PSPNet, Deeplab3+, and UperNet.

RESULTS

The test set constructed in the study achieved satisfactory results, where pixel accuracy was 99%, mean intersection over union was 0.69, negative predictive value was 98.74%, and positive predictive value was 94.27%. The model parameter was 46.38 M, the float calculation was 467.2 G, and the time length to segment and recognize a picture was 0.6 s.

CONCLUSION

Constructing a segmentation network based on deep learning to segment and recognize angiodysplasias lesions is an effective and feasible method for diagnosing angiodysplasias lesions.

Key Words: Artificial intelligence; Image segmentation; Capsule endoscopy; Angiodysplasias

©The Author(s) 2023. Published by Baishideng Publishing Group Inc. All rights reserved.

Core Tip: Small intestinal vascular malformation (vascular dysplasia) is a common cause of small intestinal bleeding. Herein, we proposed a semantic recognition segmentation network to recognize small intestinal vascular malformation lesions. This method can assist doctors in identifying lesions, improving the detection rate of intestinal vascular dysplasia, realizing automatic disease detection, and shortening the capsule endoscopy reading time.

Citation: Chu Y, Huang F, Gao M, Zou DW, Zhong J, Wu W, Wang Q, Shen XN, Gong TT, Li YY, Wang LF. Convolutional neural network-based segmentation network applied to image recognition of angiodysplasias lesion under capsule endoscopy. *World J Gastroenterol* 2023; 29(5): 879-889

URL: <https://www.wjgnet.com/1007-9327/full/v29/i5/879.htm>

DOI: <https://dx.doi.org/10.3748/wjg.v29.i5.879>

INTRODUCTION

Small intestinal vascular malformations (angiodysplasias) are common causes of small intestinal bleeding[1,2]. Angiodysplasias are degenerative lesions that manifest as abnormalities of arteries, veins, or capillaries of the original normal blood vessels. Occasionally, the term angiodysplasias include various synonymous disease concepts, such as angioectasia (AE), Dieulafoy's lesion (DL), and arteriovenous malformation. According to the Yano-Yamamoto classification, small bowel vascular lesions are classified into four types under endoscopy[3]. AE includes small erythemas and can be defined as type 1a: punctuate (< 1 mm), or type 1b: patchy (a few mm). They are characterized by thin, dilated, and tortuous veins lacking smooth muscle layers, which explain their weakness and tendency to bleed. Typically, DLs consist of small mucosal defects and can be classified as type 2a: punctuate lesions with pulsatile bleeding or type 2b: pulsatile red protrusions without surrounding venous dilatation[4]. Some arteriovenous malformations and pulsatile red protrusions with dilated peripheral veins are defined as type 3. Congenital intestinal arteriovenous malformations manifest as polypoid or cluster type[5,6] and are classified as type 4. Nevertheless, the Yano-Yamamoto classification cannot fully reflect the histopathological findings.

Capsule endoscopy (CE) is a painless and well-tolerated approach that can achieve complete visualization of the small intestine[7]. It captures images for > 8 h[8]. Previous studies have demonstrated the probability of CE diagnosis of angiodysplasias was 30%-70%, and > 50% of obscure gastrointestinal bleeding patients have angiodysplasias[9-11]. The detection rate of CE was reported to be higher than other diagnostic methods, such as small bowel computed tomography, mesenteric angiography, and enteroscopy. Therefore, using CE as a first-line inspection tool for the diagnosis of angiodysplasias is recommended[12]. Nonetheless, CE has some limitations, and only 69% of angiodysplasias can be diagnosed by gastroenterologists[13]. Less relevant lesions, such as erosions or tiny red spots, are regarded as negative results; however, distinguishing highly relevant lesions from less relevant lesions could be challenging. In addition, the diagnostic efficiency of CE decreases when the presence of bile pigments, food residues, or bubbles affects the observation of the intestinal mucosa. The doctor's manual reading of the entire gastrointestinal tract is time-consuming, and the heavy workload affects the accuracy of the diagnosis. Therefore, making diagnosis of angiodysplasias solely based on CE is challenging.

The detection rate of angiodysplasias in the small intestine can be increased by using artificial intelligence (AI) to assess the effect of automatic diagnosis, which has been successfully applied for the recognition and diagnosis of gastrointestinal endoscopic images[14]. AI assists in the recognition and diagnosis of CE images, eliminates errors in manual reading, reduces the workload of doctors, and

improves diagnosis efficiency. The clinical application of AI-based deep learning technology in wireless CE has been a research focus, which has gained increasing interest in the past two years[15-32]. Several studies[15,23-26] have used deep learning to identify ulcers from CE data. Pogorelov *et al*[27] used the color texture features to detect small intestinal bleeding in CE data. Blanes-Vidal *et al*[28] constructed a classification network to identify intestinal polyp lesions in CE data. Kundu *et al*[29] and Hajabdollahi *et al*[30] identified small bowel bleeding in CE data using a classification neural network. Obscure gastrointestinal bleeding is the main indication for small intestinal CE, and the potential risk of bleeding from vascular malformations is high[14]. Therefore, we focused on AI-assisted recognition technology for angiodysplasias in the present study. Hitherto, there are few semantic segmentation networks based on deep learning to segment and recognize angiodysplasias lesions in CE, which prompted us to introduce a segmentation model in the study. Compared with the classification model and target detection model in deep learning, the segmentation model based on deep learning can more accurately locate the focus of small intestinal vascular malformation, better assist doctors in diagnosing small intestinal vascular malformation, and improve the accuracy and efficiency of doctors' diagnosis.

Currently, significant progress has been made in semantic segmentation in the field of deep learning. To the best of our knowledge, this is the first paper that proposed using a semantic segmentation network to solve the pixel-level small intestinal vascular malformation focus recognition and location. Resnet-50 was used as the skeleton network, and the fusion mechanism based on shallow features and deep features was introduced so that the segmentation model could accurately locate the location and category of lesions. Shallow features can perceive the texture details of lesions, while deep features can perceive the semantic information between lesions. By combining these two features to segment the image, the phenomenon where the lesion area is divided into uncorrelated small areas is reduced, the pixel accuracy (PA) is improved, and the missed detection rate of the lesion is reduced. This paper introduced the proposed network structure in detail and compared three common segmentation models, *i.e.*, PSPNet[31], Deeplabv3+[32], and UperNet[33]. The obtained results confirmed that the model proposed in this paper had high-performance indicators.

MATERIALS AND METHODS

ResNet was introduced in 2015 and won first place in the classification task of the ImageNet competition on account of being "simple and practical". Afterward, many methods, which were based on ResNet50 or ResNet101, have been widely used in detection, segmentation, recognition, and other fields. This method makes a reference (X) for the input of each layer, learning to form residual functions rather than learning some functions without reference (X). This residual function is easier to optimize and can greatly deepen the number of network layers. Moreover, the extracted image features have strong robustness. ResNet50 is faster than ResNet100. Therefore, ResNet50 is selected as the skeleton network of the semantic segmentation network in this paper. Based on the fusion of shallow and deep features, Resnet-50 was used as the skeleton network to construct an improved convolutional neural network (CNN) segmentation network model that automatically recognizes the type of angiodysplasias under CE and draws the outline of the lesion in the study. The present study aimed to assist doctors in diagnosing angiodysplasias lesions with CE.

The model proposed in this study was composed of three sub-units, *i.e.*, down-sampling, up-sampling, and classifier. CE small intestine data were used as input in the module, and the final output was image lesion category information and lesion boundary information.

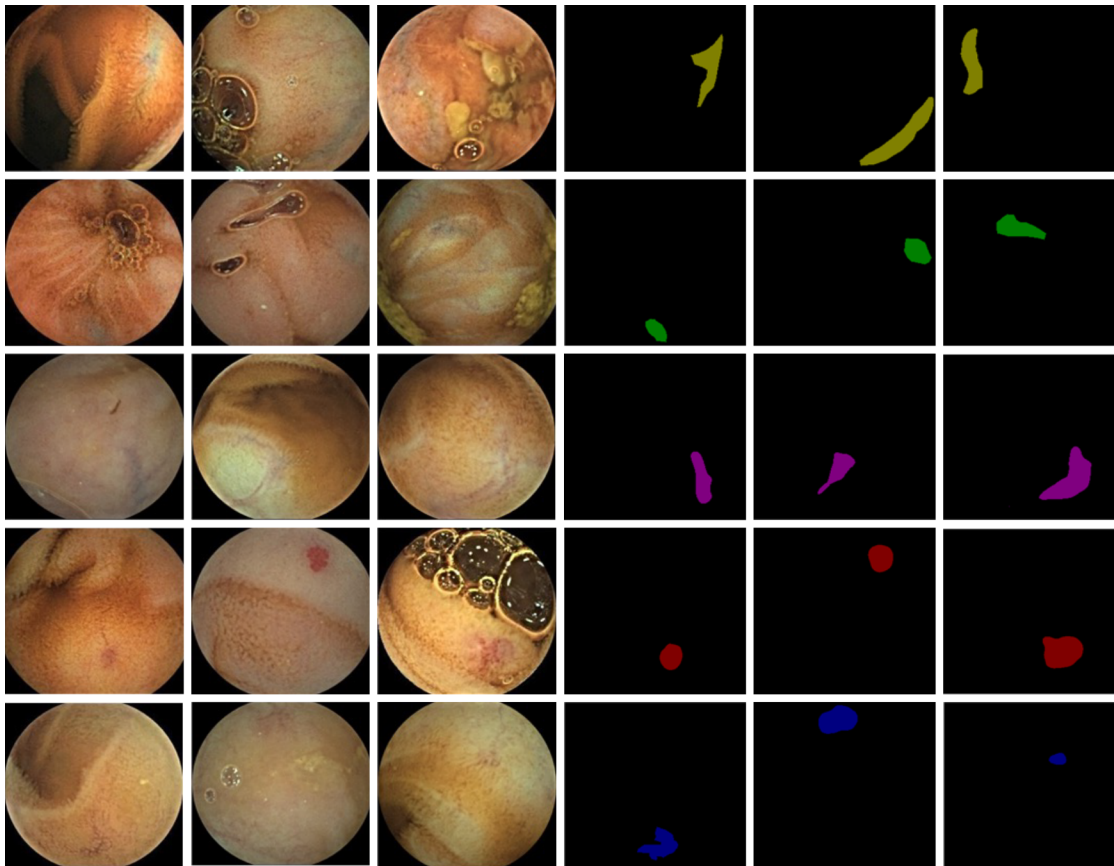
Research data set

In order to train and evaluate the segmentation model, 378 patients with angiodysplasias who underwent OMOM CE (China Chongqing Kingsoft Technology Co., Ltd) at the Ruijin Hospital between January 2014 and December 2020 were recruited in this study. The sampling frequency of OMOM capsules of 2fps, the working time of > 12 h, and the apex field of view of 150° were used to diagnose the patients. A total of 12403 pictures were identified with an image resolution of 256 × 240. The patient data were anonymized, any personal identification information was omitted, and examination information (such as examination date and patient name) was deleted from the original image. All patients provided written informed consent, and the ethics committee approved the study [the certification number was (2017) provisional ethics review No. 138]. The annotated data were marked by an experienced endoscopy group that included three experts from Ruijin Hospital Affiliated to Shanghai Jiao Tong University. The average age of the experts was 35 years, and their average CE reading experience was 5 years, with an average of 150 CE cases each year. The five types of lesions of vascular malformation were annotated, and 12403 image data and 12403 annotated mask image data were generated. The data sample map is shown in Figure 1.

This project used the image data of 178 cases as the training set and the remaining 200 cases as the test set. The training set was divided into training and verification data at a ratio of 7:3 during the training process. The test set contained 1500 images without lesions and 1500 images with lesions. The training set and test set image data are summarized in Table 1.

Table 1 Details of the training set data and test set data

Lesion type	Lesion morphology	Number of pictures/pieces	
		Training set	Test set
Telangiectasia	Red cluster	838	38
	Red spider nevus	162	4
Venous dilatation	Red branched	752	38
	Blue branched	2583	1088
Vein tumor	Blue cluster	3058	332



DOI: 10.3748/wjg.v29.i5.879 Copyright ©The Author(s) 2023.

Figure 1 Sample image of training data. The left three columns are the original image of the capsule, and the right three columns are the manual annotation results.

Data preprocessing

The training data were preprocessed to meet the requirements of the deep learning model. The preprocessing steps of the model constructed in the study were as follows: (1) Resizing the image to $256 \times 240 \times 3$; (2) using enhancement methods (rotation, flip, and tilt) on the resized image; and (3) normalizing all images. In order to train a deep learning model, the dataset was split. The dataset image was randomly divided into two parts: 70% for training and 30% for verification.

Segmentation network details

The network structure proposed in this study is shown in [Figure 2](#). The construction of the network model was inspired by the UperNet model. ResNet-50 was used as the skeleton network. The fusion mechanism of shallow features and deep features were introduced. Subsequently, the feature with the same size as the original image was obtained through the down-sampling operation. Finally, the classifier was connected to realize the pixel-level segmentation task of the image.

Based on the new semantic segmentation recognition network framework, a single end-to-end network could be trained to capture and analyze the semantic information of the CE small intestine

data. In order to fuse the shallow features and deep feature information, the last feature mapping set output by each stage in ResNet was expressed as C1, C2, C3, and C4, and the two-by-two fusion of features were utilized as down-sampling operation input, where the down-sampling rates were 4, 8, 16, and 32, respectively. The texture features of the lesion were captured at the highest layer, and the pixel-level segmentation of the lesion was completed based on the lowest layer features.

The last down-sampling operation generated a feature map with the same resolution as the original image, with a size of 256×240 . After the feature was operated by Flatten, a classifier composed of a fully connected layer was connected to complete the segmentation and recognition tasks of the capsule data.

In order to assess the fusion of features of different scales, bilinear interpolation was used to adjust them according to the size, after which a non-evolutionary layer was applied to fuse the features of different levels and reduce the channel size. All non-classifier convolutional layers underwent batch normalization Relu operations after output. The learning rate of the current iteration was equivalent to the initial learning rate multiplied by $(1 - \text{iter} / \text{max_iter_size})^{\text{power}}$, and the initial learning rate and power were set to 0.02 and 0.9, respectively.

RESULTS

Evaluation index

The performance of the segmentation model of angiodysplasias lesions in CE was evaluated based on the following indicators: Positive predictive value (PPV), negative predictive value (NPV), mean intersection over union (mIOU), and PA. PPV and NPV were calculated using formulae 1 and 2, respectively.

$$\text{PPV} = \frac{\text{TP}}{\text{TP} + \text{FP}} \quad (1)$$

$$\text{NPV} = \frac{\text{TN}}{\text{TN} + \text{FN}} \quad (2)$$

Where true positive (TP) and true negative (TN) are the true number of positive samples and the true number of negative samples, respectively; FP and FN are false positives and false negatives, respectively. IOU and mIOU calculation formulae are shown as formulae 3 and 4, respectively.

$$\text{IOU} = \frac{\text{Target area} \cap \text{Prediction area}}{\text{Target area} \cup \text{Prediction area}} \quad (3)$$

$$\text{mIOU} = \frac{1}{k+1} \sum_{i=0}^k \frac{P_{ii}}{\sum_{j=0}^k P_{ij} + \sum_{j=0}^k P_{ji} - P_{ii}} \quad (4)$$

Supposedly, there were $K+1$ categories (including an empty category or background) in semantic segmentation, which indicated that class i is predicted as i , and class j is predicted as j . The PA is calculated by formula 5.

$$\text{PA} = \frac{\sum_{i=0}^k P_{ii}}{\sum_{i=0}^k \sum_{j=0}^k P_{ij}} \quad (5)$$

Experimental design

Python 3 is a good deep-learning programming language that supports multiple deep-learning frameworks. The model was implemented using Python 3 and Torch framework. The training server has a graphics processing unit. All images were first passed to the image data generation class in Pytorch, and the preprocessing operations were performed, including enhancement, resize, and normalization operations. Then, the generated images were sent to the model to start the training. The layers in the backbone network ResNet-50 used pre-trained weights on ImageNet. An optimizer (SGD) was used to train the model, after which a weight decay of 0.0001 and a momentum of 0.9 were applied. Each model ran approximately 25000 Epochs; each Epoch iterated eight times, and the batch size was 8. In the model training process, the loss change, PA index, and mIOU changes were detected (Figure 3).

Comparison results of multiple models

On a test set consisting of 3000 image data, the following test indicators were compared on the four models: PPV, NPV, mean IOU, PA, parameter quantity, float calculation quantity, and duration. The results are shown in Table 2.

Based on the method of fusion of shallow and deep features, the CNN segmentation network model was improved and optimized, and the segmentation and recognition of five types of angiodysplasias lesions, *i.e.*, blue branch, blue cluster, red branch, red cluster, and red spider nevus, were realized. This method fully uses the shallow and deep features extracted from the skeleton network to perceive the global information and lesion texture information of the small intestine capsule image data as a whole. Thus, it significantly improves the PPV and NPV of the segmentation model in the angiodysplasias lesion image. In order to obtain the highest PPV, the NPV has to be the highest. The unified perception of the global and local information of the small intestine capsule data was completed through a CNN,

Table 2 Comparison of model accuracy

Network type	PPV (%)	NPV (%)	mIOU	PA (%)	Parameter (M)	Float calculation amount (G)	Time (s)
PSPNet	85.14	98.62	0.64	98	51.43	829.10	0.9
DeeplabV3+	45.07	99.75	0.59	89	59.34	397.00	0.95
UperNet	92.55	95.69	0.69	98	126.08	34.94	0.9
Our model	94.27	98.74	0.69	99	46.38	467.2	0.6

PPV: Positive predictive value; NPV: Negative predictive value; mIOU: Mean intersection over union; PA: Pixel accuracy.

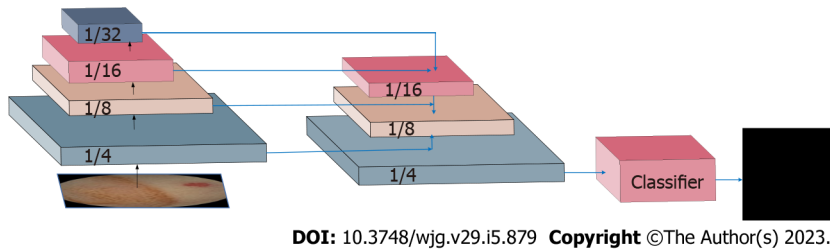


Figure 2 Network structure diagram. This figure shows the structure of semantic segmentation network, in which the first two modules are shallow and deep feature fusion, the third module is pixel classifier, and finally the network output results.

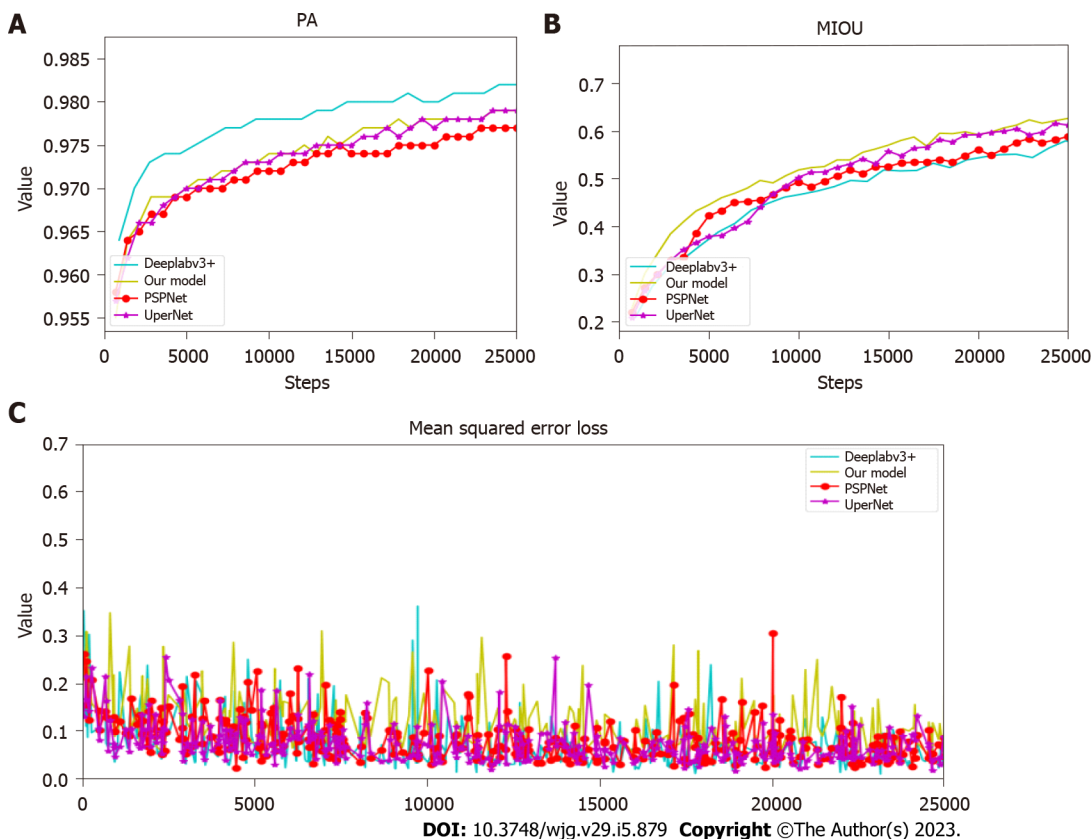


Figure 3 Change process of loss, pixel accuracy and mean intersection over union. A: Comparison of the pixel accuracy (PA) values of each model during training. The abscissa represents the number of training iterations, and the ordinate represents the value of PA; B: Comparison of the mean intersection over union (mIOU) values of each model during training. The abscissa represents the number of training iterations, and the ordinate represents the value of mIOU; C: Comparison of the loss value of each model in the training process. The abscissa represents the number of training iterations, and the ordinate represents the loss value. PA: Pixel accuracy; mIOU: Mean intersection over union.

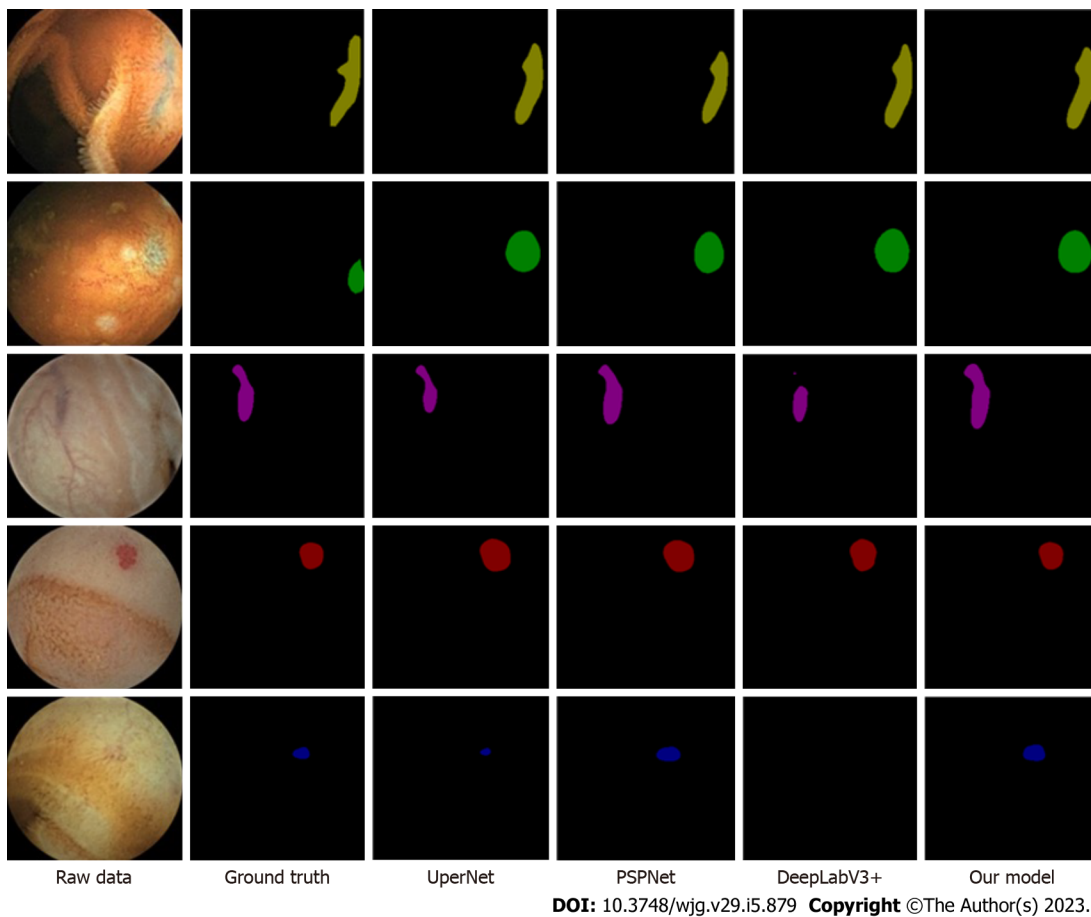


Figure 4 Five rows from top to bottom: blue branch, blue lumpy, red branch, red lumpy and red spider nevus. The first column on the left is the original image, the middle four columns are the results of the current excellent segmentation network, and the last column is the results of the model we proposed.

which reduced the number of network model parameters, the number of float calculations, and the inference time of the deep learning model. Furthermore, a comparative experiment was designed and compared to the current advanced segmentation network models: PSPNet, DeeplabV3+, and UperNet. Our model showed that the NPV reached the highest 98.74% when the PPV was the highest.

The comparison of the segmentation and recognition effects of the four models on the vascular aberration lesions of the CE small intestine data is shown in [Figure 4](#). The model proposed in the study was similar to that of the expert's annotation results.

Compared with relevant literature, Leenhardt *et al*[19] applied technology for segmentation, achieving the highest level of lesion detection, with an NPV value of 96%. However, the algorithm presented in this paper had some advantages in the test set. Also, our NPV value was 98%.

DISCUSSION

The classification network and the target detection network are the mainstream network structure that combines the deep learning model and the CE diagnosis method. In the present study, we introduced the segmentation network in deep learning, segmented and identified the angiodysplasias lesions, and completed the pixel-level segmentation task of the angiodysplasias lesions. The semantic segmentation network model had clinical practicality application as assessed using the training and test sets in comparative experiments.

The segmentation networks have been obviously developed in the field of deep learning. PSPNet uses the prior knowledge of the global feature layer to understand the semantics of various scenes, combined with the deep supervision loss to develop an effective optimization strategy on ResNet and embed difficult-to-analyze scene information features into the functional connectivity networks prediction framework to establish a pyramid. The pooling module aggregates the contextual information in different regions and improves the ability to obtain global information. This system was used for scene analysis and semantic segmentation and was 83% accurate on the COCO data set. The DeepLabV3+ model was based on an encoder-decoder structure, which improved the accuracy and saved the inference time; an accuracy rate of 89% was obtained in the COCO dataset. UperNet used

unified perception analysis to build a network with a hierarchical structure to ensure that multiple levels were resolved at visual concepts, learn the differentiated data in various image datasets, achieve joint reasoning, and explore the rich visual knowledge in the images. Finally, 79.98%-PA was obtained on the ADE20K data set. UperNet used a unified perception analysis module from scenes, objects, parts, materials, and textures to simultaneously analyze the multilevel visual concepts of images, such that many objects could be segmented and recognized, and the rate of missed objects could be reduced. The CE small intestine image data has a simple scene and fewer semantic levels. The use of large segmentation network models would cause over-fitting in training and high computational complexity. This study was inspired by UperNet and optimized basic CNN segmentation network, which led to the creation of a network model suitable for the segmentation and recognition of angiodysplasias with CE.

On the other hand, a case-based dataset encompassing typical vascular malformation images, atypical angiodysplasias images, and normal images was constructed, including pictures with poor intestinal cleanliness. According to the color and morphology of the angiodysplasias lesions in the cases, the five types of angiodysplasias lesions were summarized as blue branched, blue cluster, red branched, red cluster, and red spider nevus. The dataset constructed in this study verified the clinical applicability of the semantic segmentation model. Thus, the dataset was essential in diagnosing CE small bowel vascular malformation based on the deep learning model.

CONCLUSION

The deep learning model constructed in this study showed high PPV and NPV for the segmentation and recognition of angiodysplasias lesions. In the future, it could be used to assist capsule endoscopists in the real-time diagnosis of angiodysplasias lesions. Deep learning does not require prior knowledge, as it can directly learn the most predictive features from image data, as well as segment and recognize the image. The larger the amount of data, the higher the advantages of deep learning and the higher the recognition accuracy. AI facilitates grassroots' CE to obtain the same diagnosis effect as senior experts. However, the current uneven distribution of medical resources and the technical level of grassroots CE are the driving forces for the development of AI. In conclusion, the segmentation model based on deep learning can assist doctors in identifying the lesions of small intestinal vascular malformations.

ARTICLE HIGHLIGHTS

Research background

Small intestinal vascular malformations (angiodysplasias) commonly cause small intestinal bleeding. Therefore, capsule endoscopy has become the primary diagnostic method for angiodysplasias. Nevertheless, manual reading of the entire gastrointestinal tract is a time-consuming heavy workload, which affects the accuracy of diagnosis.

Research motivation

The doctor's manual reading of the entire gastrointestinal tract is time-consuming, and the heavy workload affects the accuracy of the diagnosis. Also, significant progress has been made in semantic segmentation in the field of deep learning.

Research objectives

This study aimed to assist in the diagnosis and increase the detection rate of angiodysplasias in the small intestine, achieve automatic disease detection, and shorten the capsule endoscopy (CE) reading time.

Research methods

A convolutional neural network semantic segmentation model with feature fusion automatically recognizes the category of vascular dysplasia under CE and draws the lesion contour, thus improving the efficiency and accuracy of identifying small intestinal vascular malformation lesions, was proposed.

Research results

The test set constructed in the study achieved satisfactory results: pixel accuracy was 99%, mean intersection over union was 0.69, negative predictive value was 98.74%, and positive predictive value was 94.27%. The model parameter was 46.38 M, the float calculation was 467.2 G, and the time needed to segment and recognize a picture was 0.6 s.

Research conclusions

Constructing a segmentation network based on deep learning to segment and recognize angiodysplasias

lesions is an effective and feasible method for diagnosing angiodysplasias lesions.

Research perspectives

The model detects the small intestinal malformation lesions in the capsule endoscopy image data and draws the lesion area through segmentation.

FOOTNOTES

Author contributions: Chu Y read and reviewed capsule endoscopy images, and participated in the design, writing, and revision of the manuscript; Huang F performed AI algorithm research, designed the segmentation recognition protocol, and verified the algorithm; Gao M organized the experimental results, visualized the experiment, and wrote the draft of the paper; Zou DW designed and revised the protocol of the paper; Zhong J reviewed capsule endoscopy images; Wu W and Wang Q participated in the reading of CE and preparation of the material; Shen XN and Gong TT partial writing of the manuscript; Li YY contributed to the coding and debugging of interface between algorithm and software; Wang LF designed and modified the protocol of the paper.

Supported by the Chongqing Technological Innovation and Application Development Project, Key Technologies and Applications of Cross Media Analysis and Reasoning, No. cstc2019jscx-zdztzxX0037.

Institutional review board statement: The study was reviewed and approved by the Ruijin Hospital Ethics Committee, Shanghai Jiao Tong University School of Medicine [the certification number was (2017) provisional ethics review No. 138].

Informed consent statement: The informed consent statement was waived by the Ruijin Hospital Ethics Committee.

Conflict-of-interest statement: The authors declare that they have no competing interests.

Data sharing statement: Technical appendix, statistical code, and dataset available from the corresponding author at lifuwang@sjtu.edu.cn. Participants gave informed consent for data sharing.

Open-Access: This article is an open-access article that was selected by an in-house editor and fully peer-reviewed by external reviewers. It is distributed in accordance with the Creative Commons Attribution NonCommercial (CC BY-NC 4.0) license, which permits others to distribute, remix, adapt, build upon this work non-commercially, and license their derivative works on different terms, provided the original work is properly cited and the use is non-commercial. See: <https://creativecommons.org/licenses/by-nc/4.0/>

Country/Territory of origin: China

ORCID number: Ye Chu 0000-0002-9204-9498; Fang Huang 0000-0002-8758-8534; Min Gao 0000-0002-4969-2488; Duo-Wu Zou 0000-0002-2461-5304; Jie Zhong 0000-0003-2919-1771; Wei Wu 0000 0001 7842 9032; Qi Wang 0000-0002-8437-8224; Xiao-Nan Shen 0000-0002-4169-3355; Ting-Ting Gong 0000-0003-1298-787X; Yuan-Yi Li 0000-0002-3180-7398; Li-Fu Wang 0000-0001-5172-9932.

S-Editor: Zhang H

L-Editor: A

P-Editor: Zhang H

REFERENCES

- 1 **Leighton JA**, Triester SL, Sharma VK. Capsule endoscopy: a meta-analysis for use with obscure gastrointestinal bleeding and Crohn's disease. *Gastrointest Endosc Clin N Am* 2006; **16**: 229-250 [PMID: 16644453 DOI: [10.1016/j.giec.2006.03.004](https://doi.org/10.1016/j.giec.2006.03.004)]
- 2 **Sakai E**, Endo H, Taniguchi L, Hata Y, Ezuka A, Nagase H, Yamada E, Ohkubo H, Higurashi T, Sekino Y, Koide T, Iida H, Hosono K, Nonaka T, Takahashi H, Inamori M, Maeda S, Nakajima A. Factors predicting the presence of small bowel lesions in patients with obscure gastrointestinal bleeding. *Dig Endosc* 2013; **25**: 412-420 [PMID: 23368528 DOI: [10.1111/den.12002](https://doi.org/10.1111/den.12002)]
- 3 **Yano T**, Yamamoto H, Sunada K, Miyata T, Iwamoto M, Hayashi Y, Arashiro M, Sugano K. Endoscopic classification of vascular lesions of the small intestine (with videos). *Gastrointest Endosc* 2008; **67**: 169-172 [PMID: 18155439 DOI: [10.1016/j.gie.2007.08.005](https://doi.org/10.1016/j.gie.2007.08.005)]
- 4 **Nguyen DC**, Jackson CS. The Dieulafoy's Lesion: An Update on Evaluation, Diagnosis, and Management. *J Clin Gastroenterol* 2015; **49**: 541-549 [PMID: 25887110 DOI: [10.1097/MCG.0000000000000321](https://doi.org/10.1097/MCG.0000000000000321)]
- 5 **Chung CS**, Chen KC, Chou YH, Chen KH. Emergent single-balloon enteroscopy for overt bleeding of small intestinal vascular malformation. *World J Gastroenterol* 2018; **24**: 157-160 [PMID: 29358892 DOI: [10.3748/wjg.v24.i1.157](https://doi.org/10.3748/wjg.v24.i1.157)]
- 6 **Molina AL**, Jester T, Nogueira J, CaJacob N. Small intestine polypoid arteriovenous malformation: a stepwise approach to diagnosis in a paediatric case. *BMJ Case Rep* 2018; **2018**: bcr2018224536 [PMID: 30042105 DOI: [10.1136/bcr-2018-224536](https://doi.org/10.1136/bcr-2018-224536)]

- 10.1136/bcr-2018-224536]
- 7 **Iddan G**, Meron G, Glukhovskiy A, Swain P. Wireless capsule endoscopy. *Nature* 2000; **405**: 417 [PMID: [10839527](#) DOI: [10.1038/35013140](#)]
 - 8 **Rondonotti E**, Spada C, Adler S, May A, Despott EJ, Koulaouzidis A, Panter S, Domagk D, Fernandez-Urien I, Rahmi G, Riccioni ME, van Hooff JE, Hassan C, Pennazio M. Small-bowel capsule endoscopy and device-assisted enteroscopy for diagnosis and treatment of small-bowel disorders: European Society of Gastrointestinal Endoscopy (ESGE) Technical Review. *Endoscopy* 2018; **50**: 423-446 [PMID: [29539652](#) DOI: [10.1055/a-0576-0566](#)]
 - 9 **Liao Z**, Gao R, Xu C, Li ZS. Indications and detection, completion, and retention rates of small-bowel capsule endoscopy: a systematic review. *Gastrointest Endosc* 2010; **71**: 280-286 [PMID: [20152309](#) DOI: [10.1016/j.gie.2009.09.031](#)]
 - 10 **Leclaire S**, Iwanicki-Caron I, Di-Fiore A, Elie C, Alhameedi R, Ramirez S, Hervé S, Ben-Soussan E, Ducrotte P, Antonietti M. Yield and impact of emergency capsule enteroscopy in severe obscure-overt gastrointestinal bleeding. *Endoscopy* 2012; **44**: 337-342 [PMID: [22389234](#) DOI: [10.1055/s-0031-1291614](#)]
 - 11 **ASGE Technology Committee**, Wang A, Banerjee S, Barth BA, Bhat YM, Chauhan S, Gottlieb KT, Konda V, Maple JT, Murad F, Pfau PR, Pleskow DK, Siddiqui UD, Tokar JL, Rodriguez SA. Wireless capsule endoscopy. *Gastrointest Endosc* 2013; **78**: 805-815 [PMID: [24119509](#) DOI: [10.1016/j.gie.2013.06.026](#)]
 - 12 **Pennazio M**, Spada C, Eliakim R, Keuchel M, May A, Mulder CJ, Rondonotti E, Adler SN, Albert J, Baltes P, Barbaro F, Cellier C, Charton JP, Delvaux M, Despott EJ, Domagk D, Klein A, McAlindon M, Rosa B, Rowse G, Sanders DS, Saurin JC, Sidhu R, Dumonceau JM, Hassan C, Gralnek IM. Small-bowel capsule endoscopy and device-assisted enteroscopy for diagnosis and treatment of small-bowel disorders: European Society of Gastrointestinal Endoscopy (ESGE) Clinical Guideline. *Endoscopy* 2015; **47**: 352-376 [PMID: [25826168](#) DOI: [10.1055/s-0034-1391855](#)]
 - 13 **Zheng Y**, Hawkins L, Wolff J, Golubeva O, Goldberg E. Detection of lesions during capsule endoscopy: physician performance is disappointing. *Am J Gastroenterol* 2012; **107**: 554-560 [PMID: [22233695](#) DOI: [10.1038/ajg.2011.461](#)]
 - 14 **Leenhardt R**, Vasseur P, Li C, Saurin JC, Rahmi G, Cholet F, Becq A, Marteau P, Histace A, Dray X; CAD-CAP Database Working Group. A neural network algorithm for detection of GI angiectasia during small-bowel capsule endoscopy. *Gastrointest Endosc* 2019; **89**: 189-194 [PMID: [30017868](#) DOI: [10.1016/j.gie.2018.06.036](#)]
 - 15 **Wang S**, Xing Y, Zhang L, Gao H, Zhang H. Deep Convolutional Neural Network for Ulcer Recognition in Wireless Capsule Endoscopy: Experimental Feasibility and Optimization. *Comput Math Methods Med* 2019; **2019**: 7546215 [PMID: [31641370](#) DOI: [10.1155/2019/7546215](#)]
 - 16 **Korman LY**, Delvaux M, Gay G, Hagenmuller F, Keuchel M, Friedman S, Weinstein M, Shetzline M, Cave D, de Franchis R. Capsule endoscopy structured terminology (CEST): proposal of a standardized and structured terminology for reporting capsule endoscopy procedures. *Endoscopy* 2005; **37**: 951-959 [PMID: [16189767](#) DOI: [10.1055/s-2005-870329](#)]
 - 17 **Gulati S**, Emmanuel A, Patel M, Williams S, Haji A, Hayee B, Neumann H. Artificial intelligence in luminal endoscopy. *Ther Adv Gastrointest Endosc* 2020; **13**: 2631774520935220 [PMID: [32637935](#) DOI: [10.1177/2631774520935220](#)]
 - 18 **Molder A**, Balaban DV, Jinga M, Molder CC. Current Evidence on Computer-Aided Diagnosis of Celiac Disease: Systematic Review. *Front Pharmacol* 2020; **11**: 341 [PMID: [32372947](#) DOI: [10.3389/fphar.2020.00341](#)]
 - 19 **Leenhardt R**, Li C, Le Mouel JP, Rahmi G, Saurin JC, Cholet F, Boureille A, Amiot X, Delvaux M, Duburque C, Leandri C, Gérard R, Leclaire S, Mesli F, Nion-Larmurier I, Romain O, Sacher-Huvelin S, Simon-Shane C, Vanbiervliet G, Marteau P, Histace A, Dray X. CAD-CAP: a 25,000-image database serving the development of artificial intelligence for capsule endoscopy. *Endosc Int Open* 2020; **8**: E415-E420 [PMID: [32118115](#) DOI: [10.1055/a-1035-9088](#)]
 - 20 **Bianchi F**, Masaracchia A, Shojaei Barjuei E, Menciassi A, Arezzo A, Koulaouzidis A, Stoyanov D, Dario P, Ciuti G. Localization strategies for robotic endoscopic capsules: a review. *Expert Rev Med Devices* 2019; **16**: 381-403 [PMID: [31056968](#) DOI: [10.1080/17434440.2019.1608182](#)]
 - 21 **Min JK**, Kwak MS, Cha JM. Overview of Deep Learning in Gastrointestinal Endoscopy. *Gut Liver* 2019; **13**: 388-393 [PMID: [30630221](#) DOI: [10.5009/gnl18384](#)]
 - 22 **Hwang Y**, Park J, Lim YJ, Chun HJ. Application of Artificial Intelligence in Capsule Endoscopy: Where Are We Now? *Clin Endosc* 2018; **51**: 547-551 [PMID: [30508880](#) DOI: [10.5946/ce.2018.173](#)]
 - 23 **Alaskar H**, Hussain A, Al-Aseem N, Liatsis P, Al-Jumeily D. Application of Convolutional Neural Networks for Automated Ulcer Detection in Wireless Capsule Endoscopy Images. *Sensors (Basel)* 2019; **19** [PMID: [30871162](#) DOI: [10.3390/s19061265](#)]
 - 24 **Wang S**, Xing Y, Zhang L, Gao H, Zhang H. A systematic evaluation and optimization of automatic detection of ulcers in wireless capsule endoscopy on a large dataset using deep convolutional neural networks. *Phys Med Biol* 2019; **64**: 235014 [PMID: [31645019](#) DOI: [10.1088/1361-6560/ab5086](#)]
 - 25 **Fan S**, Xu L, Fan Y, Wei K, Li L. Computer-aided detection of small intestinal ulcer and erosion in wireless capsule endoscopy images. *Phys Med Biol* 2018; **63**: 165001 [PMID: [30033931](#) DOI: [10.1088/1361-6560/aad51c](#)]
 - 26 **Aoki T**, Yamada A, Aoyama K, Saito H, Tsuboi A, Nakada A, Niikura R, Fujishiro M, Oka S, Ishihara S, Matsuda T, Tanaka S, Koike K, Tada T. Automatic detection of erosions and ulcerations in wireless capsule endoscopy images based on a deep convolutional neural network. *Gastrointest Endosc* 2019; **89**: 357-363.e2 [PMID: [30670179](#) DOI: [10.1016/j.gie.2018.10.027](#)]
 - 27 **Pogorelov K**, Suman S, Azmadi Hussin F, Saeed Malik A, Ostroukhova O, Riegler M, Halvorsen P, Hooi Ho S, Goh KL. Bleeding detection in wireless capsule endoscopy videos - Color versus texture features. *J Appl Clin Med Phys* 2019; **20**: 141-154 [PMID: [31251460](#) DOI: [10.1002/acm2.12662](#)]
 - 28 **Blanes-Vidal V**, Baatrup G, Nadimi ES. Addressing priority challenges in the detection and assessment of colorectal polyps from capsule endoscopy and colonoscopy in colorectal cancer screening using machine learning. *Acta Oncol* 2019; **58**: S29-S36 [PMID: [30836800](#) DOI: [10.1080/0284186X.2019.1584404](#)]
 - 29 **Kundu AK**, Fattah SA, Rizve MN. An Automatic Bleeding Frame and Region Detection Scheme for Wireless Capsule Endoscopy Videos Based on Interplane Intensity Variation Profile in Normalized RGB Color Space. *J Healthc Eng* 2018; **2018**: 9423062 [PMID: [29682270](#) DOI: [10.1155/2018/9423062](#)]
 - 30 **Hajabdollahi M**, Esfandiarpour R, Najarian K, Karimi N, Samavi S, Reza Soroushmehr SM. Low Complexity CNN Structure for Automatic Bleeding Zone Detection in Wireless Capsule Endoscopy Imaging. *Annu Int Conf IEEE Eng Med*

- Biol Soc* 2019; **2019**: 7227-7230 [PMID: 31947501 DOI: 10.1109/EMBC.2019.8857751]
- 31 **Zhao H**, Shi J, Qi X, Wang X, Jia J. Pyramid Scene Parsing Network. 2017 IEEE Conference on Computer Vision and Pattern Recognition (CVPR). Honolulu, HI, USA, 2017: 6230-6239 [DOI: 10.1109/CVPR.2017.660]
 - 32 **Chen LC**, Zhu Y, Papandreou G, Schroff F, Adam H. Encoder-Decoder with Atrous Separable Convolution for Semantic Image Segmentation. In: Ferrari V, Hebert M, Sminchisescu C, Weiss Y. Computer Vision – ECCV 2018. 2018: 833-851, Springer, Cham [DOI: 10.1007/978-3-030-01234-2_49]
 - 33 **Xiao T**, Liu Y, Zhou B, Jiang Y, Sun J. Unified Perceptual Parsing for Scene Understanding. In: Ferrari V, Hebert M, Sminchisescu C, Weiss Y. Computer Vision – ECCV 2018. 2018: 432–448, Springer, Cham [DOI: 10.1007/978-3-030-01228-1_26]



Published by **Baishideng Publishing Group Inc**
7041 Koll Center Parkway, Suite 160, Pleasanton, CA 94566, USA

Telephone: +1-925-3991568

E-mail: bpgoffice@wjgnet.com

Help Desk: <https://www.f6publishing.com/helpdesk>

<https://www.wjgnet.com>

